NEURAL REGENERATION RESEARCH
January 2016, Volume 11, Issue 1
www.nrronline.org

SPECIAL ISSUE

Magnetic resonance imaging and cell-based neurorestorative therapy after brain injury

Quan Jiang*

Department of Neurology, Henry Ford Hospital, Detroit, MI, USA

How to cite this article: *Jiang Q (2016) Magnetic resonance imaging and cell-based neurorestorative therapy after brain injury. Neural Regen Res 11(1):7-14.*

Funding: *This work was supported by NIH grants RO1 NS64134 and RO1 NS 48349.*

Abstract

Restorative cell-based therapies for experimental brain injury, such as stroke and traumatic brain injury, substantially improve functional outcome. We discuss and review state of the art magnetic resonance imaging methodologies and their applications related to cell-based treatment after brain injury. We focus on the potential of magnetic resonance imaging technique and its associated challenges to obtain useful new information related to cell migration, distribution, and quantitation, as well as vascular and neuronal remodeling in response to cell-based therapy after brain injury. The noninvasive nature of imaging might more readily help with translation of cell-based therapy from the laboratory to the clinic.

Key Words: *stroke; traumatic brain injury; traumatic brain injury; MRI; cell therapy; cell labeling; vascular remodeling; axonal remodeling; angiogenesis; neuronal plasticity; cerebral blood flow; cerebral blood volume; blood brain barrier permeability; diffusion tensor MRI*

***Correspondence to:**
Quan Jiang, Ph.D.,
qjiang1@hfhs.org.

orcid:
0000-0001-7908-4443
(Quan Jiang)

doi: *10.4103/1673-5374.169603*
http:*//www.nrronline.org/*

Accepted: *2015-03-04*

Introduction

Treatment of brain injury such as stroke and traumatic brain injury is currently either restricted to acute thrombolysis treatment with a short treatment window in stroke (NINDS, 1995), or no effective neuroprotective agents identified from traumatic brain injury clinical trials (Narayan et al., 2002). Therefore, it is important to have alternate treatment strategies with a less restrictive therapeutic window that can be applied to a large population of brain injury patients. Experimental studies in laboratory animals suggest that cell-based neurorestorative treatments may be of benefit when administered up to weeks after brain injury (Chopp and Li, 2002, 2006; Jiang et al., 2010a; Xiong et al., 2010b; Xu et al., 2013; Mouhieddine et al., 2014). The cell-based therapies that are under intense investigation include bone marrow mesenchymal cells, cord blood cells, fetal cells, and embryonic cells among others (Chopp and Li, 2002, 2006; Lindvall et al., 2004; Jiang et al., 2010a; Xiong et al., 2010b; Mouhieddine et al., 2014). In this review, we incorporate these various cell treatments under the term, cell-based therapy.

Current understanding of cell migration, distribution, angiogenesis, neurogenesis, and the interaction between angiogenesis and neurogenesis after brain injury, however, has been derived mainly from regional measurements of stained sections using histological and immunohistological methods (Auerbach et al., 2000; Zhang and Chopp, 2009; Xiong et al., 2010a; Li et al., 2014). These methods do not allow dynamic assessment of tissue remodeling, and only one measurement per experimental animal can be performed. MRI has been used to noninvasively monitor migration and distribution of magnetically labeled cells, and tissue remodeling after brain injury (Bulte et al., 2002, 2009; Hoehn et al., 2002; Frank et al., 2003; Zhang et al., 2003c; Jiang et al., 2005, 2006, 2010a; Janowski et al., 2014). In this review, we will focus on new magnetic resonance imaging (MRI) methodologies to evaluate exogenously administered cell migration, distribution and labeled cell concentration, and MRI methodologies for the detection of angiogenesis and neuronal remodeling, as primary mechanisms of injury recovery.

MRI Measurements of Migration, Distribution and Concentration of Magnetically Labeled Cells

Therapeutic benefit using neural progenitor cells depends on the migration, distribution, and concentration of the grafted cells within the target tissue (Dunnett et al., 2001; Jiang et al., 2005, 2006; Bull et al., 2014). In this section, MR labeling methods, route effects on cell migration and distribution, MRI monitoring cell migration, distribution, and concentration will be reviewed. The unresolved issues and further direction will be discussed at the end of this section.

The most critical issue for MRI monitoring cell migration and distribution is the magnetic labeling of the cells. Different MR labeling methods have been developed for different cells. The most popular way of labeling cells for treatment of brain injury is *in vitro* labeling with subsequent transplantation. The advantage of *in vitro* labeling is its optimization in iron loading with minimum effects in cell variability, cell function, and differentiation, and high specificity (Mukherjee et al., 1997; Conner and Schmid, 2003; Frank et al., 2003; Zhang et al., 2003c; Medina-Kauwe et al., 2005).

There are several other approaches for labeling cells (Hinds et al., 2003; Zhang et al., 2003c; Crich et al., 2004; Ho and Hitchens, 2004; Shapiro et al., 2005), and the most widely used method for cell labeling is dextran-coated superparamagnetic iron oxide with transfer agents. Superparamagnetic iron oxide using transfer agents are stably incorporated into cells with minimum side effects and have shown successful MRI monitoring ability (Bulte et al., 2001, 2002, 2003, 2009; Hoehn et al., 2002; Bulte and De Cuyper, 2003; Frank et al., 2003, 2004; Arbab et al., 2004, 2005; Bulte and Kraitchman, 2004; Janowski et al., 2014). The technique has been introduced into the clinic (Bulte, 2009).

The route of administration of cells is another important parameter for cell treatment of brain injury (Li et al., 2010). Currently, several routes have been used to administer cells, including intraparenchymal injection, intracerebral, intracisternal, intravenous, and intra-arterial. Intraparenchymal stereotactic cell injection is the insertion of a needle and infusion of the cells into the brain parenchyma. Intraparenchymal injections can be precisely targeted towards the lesion; however, this method is invasive. There is usually poor cell distribution through the lesion and limited migratory potential of injected cells in ischemic brain (O'Leary and Blakemore, 1997; Li et al., 2000; Lu et al., 2001; Hoehn et al., 2002; Zhang et al., 2003b). Intracisternal injection of cells enables widespread cerebral engraftment of cells along the cerebrospinal fluid from spinal to ischemic damaged tissue. The injected cells will cross the blood-cerebrospinal fluid barrier to penetrate into the parenchyma. We have investigated the migration and distribution of subventricular zone cells transplanted intracisternally into rat brain. The advantage of intracisternal administration is that it permits dynamic monitoring of cell migration from injection site to final targets as demonstrated in **Figure 1** and for the delivery of subventricular zone cells which are accustomed to the cerebrospinal fluid environment (Zhang et al., 2003b). Intracisternal injection not only provides information on the migration and distribution of the labeled cells but also on the migration speed of the labeled cells. The mean speed of labeled subventricular zone cell movement from the injection site to the parenchyma is 65 ± 14.6 m/h, which is comparable to published data (Alvarez-Buylla et al., 2000). Intra-arterial injection can be used to bypass the initial uptake by the systemic organs and deliver larger numbers of cells directly to the ischemic lesion, once vessels are reperfused (Li et al., 2001, 2010; Lu et al., 2001; Walczak et al., 2008). However, intra-arterial injection may involve a relatively high mortality rate in animals (Walczak et al., 2008). Intravenous injection is a relatively easy and the least invasive procedure for cell delivery. Intravenous injection allows broad distribution of cells within the target ischemic tissue. However, intravenous injection causes the cells to first distribute through the body, with many cells accumulating and trapped in filtering organs such as the lungs and liver. Therefore, intravenous injection may lead to low numbers of cells at the lesion.

MRI can monitor migration and distribution of magnetically labeled cells in the brain after transplantation. However, quantitative determination of labeled cells remains a challenge, especially *in vivo*. Assessment of brain iron has typically involved the measurement of proton transverse relaxation rate, R_2 ($1/T_2$; **Table 1**) (Bizzi et al., 1990; Schenker et al., 1993; Ordidge et al., 1994; Vymazal et al., 1995a, b, 1996). Several authors have observed a relationship between transverse relaxation rate (R_2) and labeled cell concentration *in vitro* (Zelivyanskaya et al., 2003). However, the relationship between R_2 and labeled cell concentration is much more complicated *in vivo* and has not been well studied. Additionally, the theory establishing the relationship between R_2 and labeled cell concentration, especially the effects of diffusion, has not been formulated. One recent study tested a theory relating R_2 and apparent diffusion coefficient (ADC) to labeled cell concentration (Athiraman et al., 2009). Experimental tests were performed both *in vitro* and *in vivo*. The data demonstrate that R_2, ADC, and ADC × R_2 has a linear relationship with labeled cell concentration *in vitro* and that multiple factors have to be considered when these relationships are evaluated *in vivo*, especially the background variation caused by ischemic damage (Athiraman et al., 2009).

There are several unresolved issues in the field for evaluating cell distribution and concentration. The labeled cells maybe die, proliferate, divide, or the magnetic labeled particles from died cells may be eaten by macrophages after administration which could lead to error massage in cell distribution and concentration. Current methods for evaluating cell concentration are more suitable for acute time (days) but not yet for chronic (weeks or months) monitoring. Chronic monitoring of cell distribution and concentration needs to resolve more issues related to cell death, proliferation, division, or labeled macrophages. The potential advanced MRI method to evaluate labeled cell concentration may be quantitative susceptibility mapping (**Table 1**) which could reduce the background variation to estimate labeled cell concentration more accurately (Kressler et al., 2010; Haacke et al., 2015).

MRI Measurements of Vascular Remodeling after Brain Injury

Angiogenesis is a primary factor associated with improved neurological recovery after brain injury (Weiller et al., 1993; Cramer et al., 1997). Patients with a higher cerebral blood vessel density after brain injury make better progress and survive longer than patients with lower vascular density (Krupinski et al., 1994; Slevin et al., 2000). Preclinical studies in brain injury indicate that neurological improvement after brain injury is induced by cell-based treatments that induce angiogenesis (Chopp et al., 2000; Chen et al., 2001; Zhang et al., 2002a, 2003a, 2005). Thus, enhanced angiogenesis observed after treatment with cell-based therapy may contribute to functional improvement. Several pre-clinical studies demonstrated that treatment of brain injury in rats with cell-based therapy increased levels of rat vascular endothelial growth factor (Zhang et al., 2002c, 2003a), which consequently enhances angiogenesis and reduces functional deficits (Chopp et al., 2000; Zhang and Chopp, 2009; Xiong et al., 2010a). Based on histopathological investigation of

angiogenesis after brain injury, MRI methodologies have been developed and implemented to monitor the spatial and temporal evolution of vascular remodeling. Angiogenesis and vasculogenesis are complex processes by which new capillaries form by sprouting from pre-existing vessels or de novo, respectively (Risau, 1998). These newly formed cerebral vessels are inherently leaky, as it can take several weeks to form a functional blood brain barrier (BBB) (Risau, 1994). Monitoring changes in blood volume over time may reflect the growth of new blood vessels and, therefore, may reflect angiogenesis and vasculogenesis (Hawighorst et al., 1998a, b; Brasch and Turetschek, 2000; Pathak et al., 2001). A significant correlation was found between dynamic contrast enhanced MRI blood volume measurements and histological determination of microvessel density in angiogenic hotspots (Hawighorst et al., 1998a, b; Brasch and Turetschek, 2000; Pathak et al., 2001). A link between angiogenesis and vascular permeability has been established through the work of Dvorak on vascular endothelial growth factor (Dvorak et al., 1999). MRI in combination with 3D laser scanning confocal microscopy images of neural progenitor cell therapy of stroke in rats has shown significant correlations between angiogenesis and increased cerebral blood flow (**Table 1**), cerebral blood volume and blood-to-brain transfer constant (K_i) for gadolinium-diethylanetriamine penta-acetic acid (Gd-DTPA) (Zhang et al., 2002b; Jiang et al., 2005). These MR measurements identify the location and area of vascular remodeling and angiogenesis (**Figure 2**) (Jiang et al., 2005).

In addition to cerebral blood flow, cerebral blood volume and Ki MRI measurements of angiogenesis after brain injury, susceptibility weighted imaging (SWI; **Table 1**) incorporating phase information also exhibited high sensitivity in detecting angiogenesis (Ding et al., 2008; Jiang et al., 2008). Because angiogenesis typically occurs in regions of high oxygen extraction, SWI will generate early images of small draining veins in peri-infarct regions that are likely to promote angiogenesis. Combination of SWI and K_i may also provide information about the stage of angiogenesis (Ding et al., 2008; Jiang et al., 2008). These MRI measurements also offer an indirect means of detecting newly formed vessels. Angiogenesis evokes an increase in microvessel density (MVD; **Table 1**). Several authors have used MRI to estimate vessel size, and this can be correlated with blood volume as a means of inferring microvessel density (Wu et al., 2004). The ratio of changes in gradient-echo to spin-echo relaxation rate ($\Delta R2^*/\Delta R_2$) induced by a high molecular weight intravascular contrast agent may provide an indication of average vessel size in a voxel under certain conditions related to echo time, contrast concentration and the main magnetic field (Boxerman et al., 1995; Dennie et al., 1998). $\Delta R2^*/\Delta R_2$ is a dimensionless ratio, and its expression in terms of tissue model parameters depends on not only vessel size distribution but also contrast concentration and the water diffusion coefficient (Jensen and Chandra, 2000). To avoid strong dependency on contrast concentration, Jensen and Chandra suggested using the quantity $Q \equiv \Delta R_2/(\Delta R_2^*)^{2/3}$ an analytic parameter that involves only intrinsic properties of the vascular network, which is sensitive to vessel density but not size (Jensen and Chandra, 2000). MRI measurement of MVD, mean segment length (MSL) and vessel size index (VSI) has been recently applied to angiogenesis during recovery of brain injury (Bosomtwi et al., 2008, 2011). By direct comparison of MVD, MSL, and VSI measured between MRI corresponding immunostained sections, a good agreement in the intracorrelation coefficient (ICC) and correlation were observed in the recovery region and normal contralateral hemisphere (Bosomtwi et al., 2008, 2011). MRI MVD, MSL, and VSI measurements exhibit promise for quantitative evaluation of microvascular changes in the brain tissue after injury. Further investigation of MRI methodologies in evaluating vascular remodeling after brain injury may focus on translation to clinic with shortest data acquisition time and maximize information.

MRI Measurements of Neuronal Remodeling after Brain injury

In addition to vascular changes, cell-based therapy also enhances neuronal remodeling, *e.g.*, promoting axonal growth and remyelination, new axonal sprouting, synaptogenesis, and endogenous neurogenesis, all of which contribute to functional recovery (Chopp et al., 2008; Zhang and Chopp, 2009; Jiang et al., 2010b; Chen et al., 2014). Cell-based treatment of stroke significantly increases both progenitor and mature oligodendrocytes in the ipsilateral hemisphere of the ischemic brain (Li et al., 2005; Zhang et al., 2013). Oligodendrocytes generate myelin and contribute to the integrity of white matter tracks in the brain. Stimulation and amplification of these cells may lead to restructuring of axons and myelin. White matter architecture in the ischemic boundary was altered by the cell treatment, and axonal density in the peri-infarct area was significantly increased in the treated animals. Pseudorabies virus labeled with green fluorescent protein (PRV-GFP) and red fluorescent protein (PRV-RFP) has been used to identify axonal remodeling in experimental stroke animal model (Liu et al., 2007). In normal rats, without stroke, few cells were labeled green in the left pyramidal neurons. After stroke, there is a significant increase in green and yellow pyramidal neurons, indicating ipsilateral or transcallosal rewiring (Liu et al., 2007). Treatment with MSCs brought a significant increase in green and yellow pyramidal cells in the left hemisphere. Comparable cross rewiring is also present in the ipsilateral hemisphere. These data indicate that treatment of brain injury with MSCs creates new circuitry in both the ipsilateral and contralateral hemispheres. Response to treatment of brain injury with MSCs also extends beyond the brain to the spinal cord (Liu et al., 2007).

MRI has demonstrated an unprecedented ability to obtain structural and physiologic information of the brain. Diffusion tensor MRI (DTI) provides a means for delineating the anatomic connectivity of white matter pathways and can be used to detect pathologic tract disruption based on the movement of water. DTI provides us two scalars called apparent diffusion coefficient (ADC) and fractional anisotropy

Table 1 Advantage and disadvantage of magnetic resonance imaging (MRI) measurements

MRI measurements	Advantage	Disadvantage
Labeled cells:		
-T2 and T2*	-Quantitative map	-Low resolution and involved error in evaluating cell concentration
-Quantitative susceptibility mapping	-Quantitative map and excellent to evaluate cell concentration	-Complex analysis and low signal to noise
Vascular remodeling:		
-Cerebral blood flow and cerebral blood volume	-Clinical available measurements	-Low sensitivity
-Susceptibility weighted imaging	-High resolution to identify vessels	-Not a quantitative map
-K_i	-High sensitivity to identify immature new vessels	-Low resolution and signal to noise
-Microvessel density, mean segment length, and vessel size index	-Quantitative map of microvasculature	-Low resolution and signal to noise
Neuronal remodeling:		
-Fractional anisotropy and fiber tracking	-Clinical available measurements	-Involved error due to modeling
-Apparent kurtosis coefficient	-Quantitative map of diffusion distribution	-Not a physiological map
-Axonal density	-Quantitative map of axonal density	-Complex analysis and low signal to noise

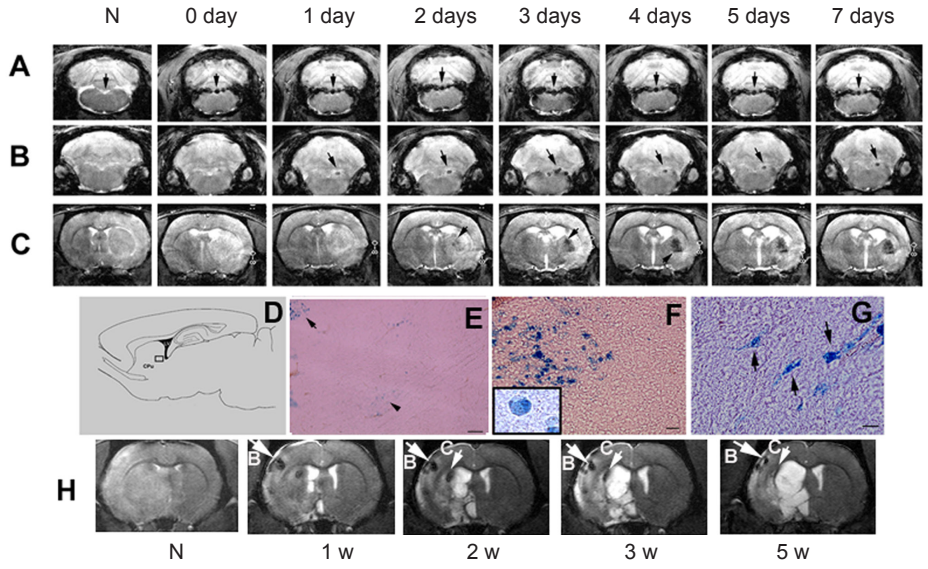

Figure 1 Dynamic migration of transplanted cells in ischemic brain in a representative ischemic rat.
MRI signals (dark areas) were not detected before transplantation of labeled subventricular zone cells (column N in A to C). In contrast, the same rat exhibited magnetic resonance imaging (MRI) signals at the fourth ventricle at the day of injection of superparamagnetic labeled cells into the cistern (A; 0 d, arrow). MRI signals moved forward along the fourth ventricle 1 and 2 days (B; 1 d and 2 d, arrows) and first reached the ipsilateral striatum nearby the ipsilateral lateral ventricle 2 days after transplantation (C; 2 d, arrow). MRI signals expanded from nearby the lateral ventricle to the distant lateral ventricle in the ipsilateral hemisphere 4 days after transplantation (C; 4 d, arrow), and MRI signal in the ipsilateral striatum increased from 2 to 4 days after transplantation (C; 5 d and 7 d). MRI signals were not detected in the contralateral hemisphere at any time points after transplantation (C; 0 d to 7 d). Panels A to C represent different levels of coronal sections from the posterior to anterior brain (A, bregma _13.3 mm; B, bregma _11.8 mm; and C, bregma_1.3 mm). N represents 1 day before transplantation, and 0 d to 7 d indicate days after transplantation from a representative rat. Prussian blue staining was used to identify superparamagnetic labeled cells on sagittal or coronal sections. This staining reacts with iron to produce blue color. Panel D is a schematic representation of a sagittal section from the ipsilateral hemisphere at lateral 1.40 mm. Panels E to G are microphotographic images of Prussian blue-stained sections from the same rat in which MRI images were presented above. Panel E is from the boxed area in the panel D. The arrow in the panel E indicates transplanted cells (blue) around the ischemic boundary. Higher magnification showed that these blue cells had round morphology (F and inset). A box and an arrowhead in panel E show transplanted cells at a distance from the ischemic boundary, and these cells exhibited bipolar morphology (G), indicating that these cells migrate. Panel H shows that MRI signals (arrows) from a representative rat localized to the boundary regions of the ischemic lesion and persisted for at least 5 weeks after transplantation. N represents 1 day before transplantation, and 1 W to 5 W indicate weeks after transplantation. Reprint from Ann Neurol, 2003;53:259-263, with permission.

(FA; **Table 1**) (Conturo et al., 1996; Shimony et al., 1999), which characterize the magnitude of water diffusion and the degree of anisotropy, respectively, for each voxel. In addition, axial (parallel to long axis of fiber) and radial (perpendicular) diffusivity are given by corresponding eigenvector values which may be related to axonal (axial diffusivity) or myelination (radial diffusivity) status (Song et al., 2002; Sun et al., 2006). FA is directly correlated with histological markers of myelination (Watanabe et al., 2001; Beaulieu, 2002; Mori and van Zijl, 2002; Sotak, 2002). Increased FA appears to correlate with white matter tract integrity, while reduced FA is correlated with functional deficits (Watanabe et al., 2001; Beaulieu, 2002; Sotak, 2002). Recent studies have shown that restorative treatment of brain injury promotes axonal remodeling and increases oligodendrocytes (remyelination) (Li et al., 2005; Shen et al., 2006). FA may be able to identify

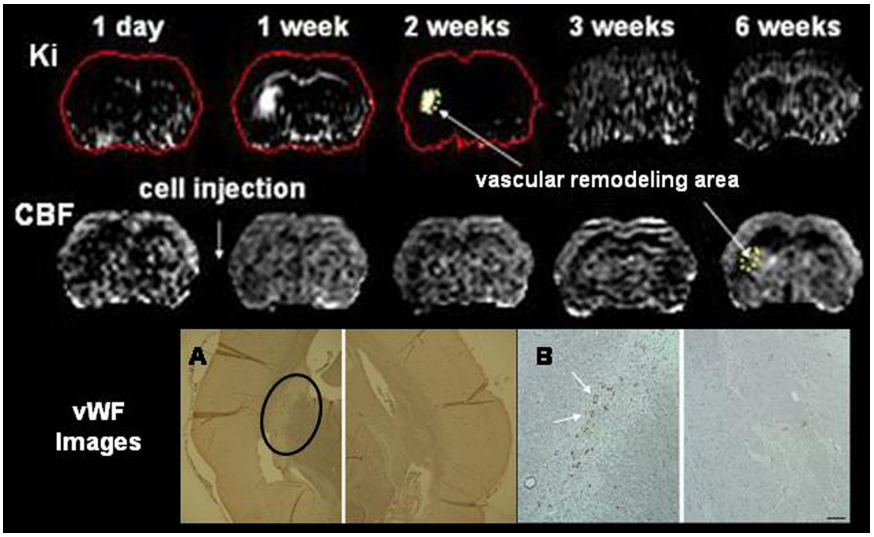

Figure 2 The evolution of changes in MRI K_i and CBF after restorative cell treatment.
The K_i maps revealed an increase in K_i in the subcortical region (yellow dotted circle) that maximized at 2 weeks (K_i, 2 weeks) and returned to normal 6 weeks after treatment. Panels A and B show the vWF immunoreactive images of coronal sections, which matched MRI sections from the same animal sacrificed at 6 weeks after treatment. The data show increased numbers of vWF immunoreactive vessels (left image in A, black line area; left image in the magnified vWF immunostained image B, arrows). The density of microscopic vessels was significantly higher in cell treated animals than in control animals, indicating that the cell therapy enhances vascular remodeling. CBF measurements revealed a small and gradual increase in the subcortical region (yellow dotted circle), where increased numbers of microvessels were confirmed by histology, starting at 3 weeks and with increased contrast at 6 weeks after treatment. By statistical analysis, vascular remodeling was coincident with increases of CBF and CBV (CBF, $P < 0.01$; CBV, $P < 0.01$) at 6 weeks after treatment, and coincident with transient increases ($P < 0.05$) of K_i with a peak at 2–3 weeks after cell therapy (Jiang et al., 2005). Bar in B: 100 μm. Reprint from Neuroimage, 2005;28:698-707, with permission. MRI: Magnetic resonance imaging; vWF: von Willebrand factor; CBF: cerebral blood flow; CBV: cerebral blood volume.

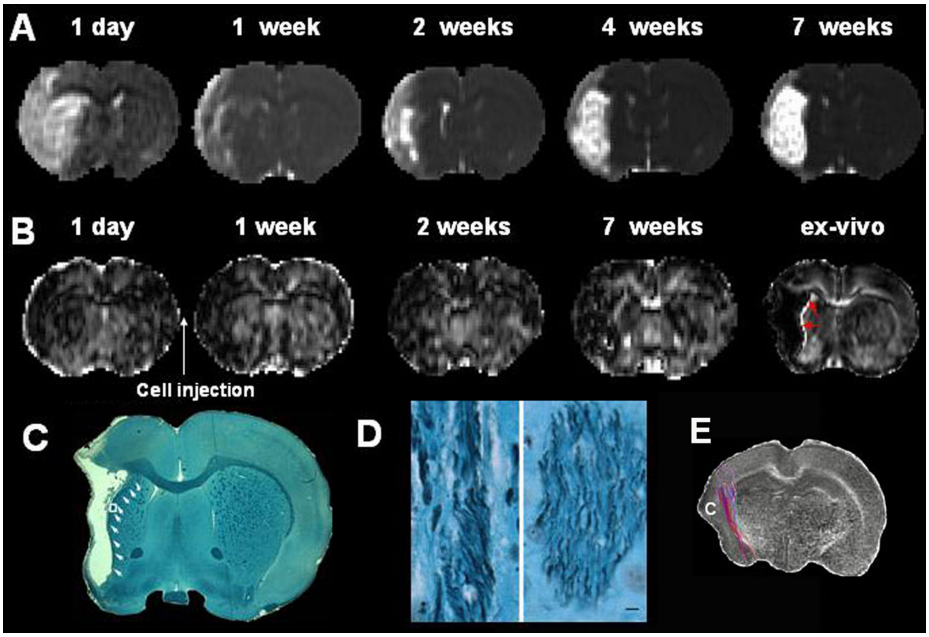

Figure 3 The evolution in T2 (A) and fractional anisotropy (B) maps after neural progenitor cell treatment and corresponding Bielshowsky silver and Luxol fast blue stained coronal section (C, D) from the same rat.
The left image in D is a high magnification image from the box area in panel C and the corresponding contralateral area (right image in D). E is the axonal tracking image from *ex vivo* diffusion tensor imaging data of another rat which show that fiber tracks circumscribe the lesion boundary. The marker C in E represents ischemic core. The bar in D: 10 μm. Reprint from Neuroimage, 2006;32:1080-1089, with permission.

ischemia injured cerebral tissue undergoing white matter reorganization after restorative treatment. The immunoreactive staining profile showed that axonal projections emanating from individual parenchymal neurons exhibited an overall orientation parallel to the lesion areas after stroke (Li et al., 2005; Jiang et al., 2006).

We have demonstrated that white matter reorganization, confirmed by an increase in axons and myelination, after neural progenitor cell treatments is coincident with increases of FA (**Figure 3**; red arrows) in the ischemic recovery regions (Jiang et al., 2006). Also the fiber tracking maps derived from diffusion tensor imaging revealed that axonal projections emanating from individual parenchymal neurons exhibited an overall orientation parallel to lesion areas (E, red lines) after stroke similar to the orientation patterns as the immunohistological results (D). So far, conventional DTI is still dominant in the investigation of white matter damage and reorganization. However, when white matter fiber tracts

cross, conventional DTI, produces an anomalous result, showing an overall lowering of FA despite the presence of highly-oriented tissue. The inability of conventional DTI to resolve multiple fiber directions derives from the assumption of Gaussian diffusion inherent to the tensor model (Basser et al., 2000; Alexander et al., 2002; Tuch et al., 2002). The distribution of the path of water molecules for the time of the MRI experiment can be generated through q-space DTI (q-DTI), including diffusion spectrum imaging (Wedeen et al., 2005), q-ball (Tuch et al., 2003), persistent angular structure MRI (PASMRI) (Alexander, 2005), and diffusion kurtosis imaging. Characterization of white matter tracts using q-DTI will provide more mechanistic information between white matter remodeling and functional recovery after traumatic brain injury. Recent investigation has demonstrated that the apparent kurtosis coefficient (AKC; **Table 1**) detected additional axonal remodeling regions with crossing axons confirmed by immunohistological staining compared with FA (Jiang et al., 2011). Further investigation of MRI methodologies in evaluating axonal changes after brain injury may focus on quatitation of axonal density (Jespersen et al., 2010; Wang et al., 2013; Davoodi-Bojd et al., 2014), myelin contents (Davoodi-Bojd and Soltanian-Zadeh, 2011; Melbourne et al., 2013; Ganzetti et al., 2014) and axonal permeability (Davoodi-Bojd et al., 2014).

Conclusion

We have demonstrated that MRI can be used to visualize cell migration, distribution, and determine labeled cell concentration as well as to monitor mechanisms related to brain injury recovery with cell-based treatment. Cell-based therapy can enhance the endogenous restorative mechanisms of the injured brain and amplify angiogenesis and axonal remodeling. Based on the mechanism of recovery from brain injury, MRI methodologies can be employed to dynamically characterize spatio-temporal events related to brain remodeling. Since the noninvasive nature of MRI methodologies allows us to translate MRI methodologies from animal to patient, MRI technique for studying cell therapy induced recovery from brain injury could lead to optimization of cell transplantation protocols and improved management of brain injury.

References

Alexander DC (2005) Multiple-fiber reconstruction algorithms for diffusion MRI. Ann N Y Acad Sci 1064:113-133.

Alexander DC, Barker GJ, Arridge SR (2002) Detection and modeling of non-Gaussian apparent diffusion coefficient profiles in human brain data. Magn Reson Med 48:331-340.

Alvarez-Buylla A, Herrera DG, Wichterle H (2000) The subventricular zone: source of neuronal precursors for brain repair. Prog Brain Res 127:1-11.

Arbab AS, Yocum GT, Rad AM, Khakoo AY, Fellowes V, Read EJ, Frank JA (2005) Labeling of cells with ferumoxides-protamine sulfate complexes does not inhibit function or differentiation capacity of hematopoietic or mesenchymal stem cells. NMR Biomed 18:553-559.

Arbab AS, Yocum GT, Kalish H, Jordan EK, Anderson SA, Khakoo AY, Read EJ, Frank JA (2004) Efficient magnetic cell labeling with protamine sulfate complexed to ferumoxides for cellular MRI. Blood 104:1217-1223.

Athiraman H, Jiang Q, Ding GL, Zhang L, Zhang ZG, Wang L, Arbab AS, Li Q, Panda S, Ledbetter K, Rad AM, Chopp M (2009) Investigation of relationships between transverse relaxation rate, diffusion coefficient, and labeled cell concentration in ischemic rat brain using MRI. Magn Reson Med 61:587-594.

Auerbach JM, Eiden MV, McKay RD (2000) Transplanted CNS stem cells form functional synapses in vivo. Eur J Neurosci 12:1696-1704.

Basser PJ, Pajevic S, Pierpaoli C, Duda J, Aldroubi A (2000) In vivo fiber tractography using DT-MRI data. Magn Reson Med 44:625-632.

Beaulieu C (2002) The basis of anisotropic water diffusion in the nervous system - a technical review. NMR Biomed 15:435-455.

Bizzi A, Brooks RA, Brunetti A, Hill JM, Alger JR, Miletich RS, Francavilla TL, Di Chiro G (1990) Role of iron and ferritin in MR imaging of the brain: a study in primates at different field strengths. Radiology 177:59-65.

Bosomtwi A, Chopp M, Zhang L, Zhang ZG, Lu M, Jiang Q (2011) Mean microvessel segment length and radius after embolic stroke: Comparison of magnetic resonance imaging (MRI) and laser scanning confocal microscopy (LSCM). Brain Res 1381:217-227.

Bosomtwi A, Jiang Q, Ding GL, Zhang L, Zhang ZG, Lu M, Ewing JR, Chopp M (2008) Quantitative evaluation of microvascular density after stroke in rats using MRI. J Cereb Blood Flow Metab 28:1978-1987.

Boxerman JL, Hamberg LM, Rosen BR, Weisskoff RM (1995) MR contrast due to intravascular magnetic susceptibility perturbations. Magn Reson Med 34:555-566.

Brasch R, Turetschek K (2000) MRI characterization of tumors and grading angiogenesis using macromolecular contrast media: status report. Eur J Radiol 34:148-155.

Bull E, Madani SY, Sheth R, Seifalian A, Green M, Seifalian AM (2014) Stem cell tracking using iron oxide nanoparticles. Int J Nanomedicine 9:1641-1653.

Bulte JW (2009) In vivo MRI cell tracking: clinical studies. AJR Am J Roentgenol 193:314-325.

Bulte JW, De Cuyper M (2003) Magnetoliposomes as contrast agents. Methods Enzymol 373:175-198.

Bulte JW, Kraitchman DL (2004) Iron oxide MR contrast agents for molecular and cellular imaging. NMR Biomed 17:484-499.

Bulte JW, Duncan ID, Frank JA (2002) In vivo magnetic resonance tracking of magnetically labeled cells after transplantation. J Cereb Blood Flow Metab 22:899-907.

Bulte JW, Ben-Hur T, Miller BR, Mizrachi-Kol R, Einstein O, Reinhartz E, Zywicke HA, Douglas T, Frank JA (2003) MR microscopy of magnetically labeled neurospheres transplanted into the Lewis EAE rat brain. Magn Reson Med 50:201-205.

Bulte JW, Douglas T, Witwer B, Zhang SC, Strable E, Lewis BK, Zywicke H, Miller B, van Gelderen P, Moskowitz BM, Duncan ID, Frank JA (2001) Magnetodendrimers allow endosomal magnetic labeling and in vivo tracking of stem cells. Nat Biotechnol 19:1141-1147.

Chen J, Venkat P, Zacharek A, Chopp M (2014) Neurorestorative therapy for stroke. Front Hum Neurosci 8:382.

Chen J, Li Y, Wang L, Zhang Z, Lu D, Lu M, Chopp M (2001) Therapeutic benefit of intravenous administration of bone marrow stromal cells after cerebral ischemia in rats. Stroke 32:1005-1011.

Chopp M, Li Y (2002) Treatment of neural injury with marrow stromal cells. Lancet Neurol 1:92-100.

Chopp M, Li Y (2006) Transplantation of bone marrow stromal cells for treatment of central nervous system diseases. Adv Exp Med Biol 585:49-64.

Chopp M, Li Y, Zhang J (2008) Plasticity and remodeling of brain. J Neurol Sci 265:97-101.

Chopp M, Zhang XH, Li Y, Wang L, Chen J, Lu D, Lu M, Rosenblum M (2000) Spinal cord injury in rat: treatment with bone marrow stromal cell transplantation. Neuroreport 11:3001-3005.

Conner SD, Schmid SL (2003) Regulated portals of entry into the cell. Nature 422:37-44.

Conturo TE, McKinstry RC, Akbudak E, Robinson BH (1996) Encoding of anisotropic diffusion with tetrahedral gradients: a general mathematical diffusion formalism and experimental results. Magn Reson Med 35:399-412.

Cramer SC, Nelles G, Benson RR, Kaplan JD, Parker RA, Kwong KK, Kennedy DN, Finklestein SP, Rosen BR (1997) A functional MRI study of subjects recovered from hemiparetic stroke. Stroke 28:2518-2527.

Crich SG, Biancone L, Cantaluppi V, Duo D, Esposito G, Russo S, Camussi G, Aime S (2004) Improved route for the visualization of stem cells labeled with a Gd-/Eu-chelate as dual (MRI and fluorescence) agent. Magn Reson Med 51:938-944.

Davoodi-Bojd E, Soltanian-Zadeh H (2011) Evaluation of diffusion models of fiber tracts using diffusion tensor magnetic resonance imaging. Magn Reson Imaging 29:1175-1185.

Davoodi-Bojd E, Chopp M, Soltanian-Zadeh H, Wang S, Ding G, Jiang Q (2014) An analytical model for estimating water exchange rate in white matter using diffusion MRI. PLoS One 9:e95921.

Dennie J, Mandeville JB, Boxerman JL, Packard SD, Rosen BR, Weisskoff RM (1998) NMR imaging of changes in vascular morphology due to tumor angiogenesis. Magn Reson Med 40:793-799.

Ding G, Jiang Q, Li L, Zhang L, Zhang ZG, Ledbetter KA, Gollapalli L, Panda S, Li Q, Ewing JR, Chopp M (2008) Angiogenesis detected after embolic stroke in rat brain using magnetic resonance T2*WI. Stroke 39:1563-1568.

Dunnett SB, Bjorklund A, Lindvall O (2001) Cell therapy in Parkinson's disease - stop or go? Nat Rev Neurosci 2:365-369.

Dvorak HF, Nagy JA, Feng D, Brown LF, Dvorak AM (1999) Vascular permeability factor/vascular endothelial growth factor and the significance of microvascular hyperpermeability in angiogenesis. Curr Top Microbiol Immunol 237:97-132.

Frank J, Anderson SA, Arbab AS (2007) Methods for labeling nonphagocytic cells with MR contrast agents. New York: CRC Press.

Frank JA, Anderson SA, Kalsih H, Jordan EK, Lewis BK, Yocum GT, Arbab AS (2004) Methods for magnetically labeling stem and other cells for detection by in vivo magnetic resonance imaging. Cytotherapy 6:621-625.

Frank JA, Miller BR, Arbab AS, Zywicke HA, Jordan EK, Lewis BK, Bryant LH, Jr., Bulte JW (2003) Clinically applicable labeling of mammalian and stem cells by combining superparamagnetic iron oxides and transfection agents. Radiology 228:480-487.

Ganzetti M, Wenderoth N, Mantini D (2014) Whole brain myelin mapping using T1- and T2-weighted MR imaging data. Front Hum Neurosci 8:671.

Haacke EM, Liu S, Buch S, Zheng W, Wu D, Ye Y (2015) Quantitative susceptibility mapping: current status and future directions. Magn Reson Imaging 33:1-25.

Hawighorst H, Weikel W, Knapstein PG, Knopp MV, Zuna I, Schonberg SO, Vaupel P, van Kaick G (1998a) Angiogenic activity of cervical carcinoma: assessment by functional magnetic resonance imaging-based parameters and a histomorphological approach in correlation with disease outcome. Clin Cancer Res 4:2305-2312.

Hawighorst H, Knapstein PG, Knopp MV, Weikel W, Brix G, Zuna I, Schonberg SO, Essig M, Vaupel P, van Kaick G (1998b) Uterine cervical carcinoma: comparison of standard and pharmacokinetic analysis of time-intensity curves for assessment of tumor angiogenesis and patient survival. Cancer Res 58:3598-3602.

Hinds KA, Hill JM, Shapiro EM, Laukkanen MO, Silva AC, Combs CA, Varney TR, Balaban RS, Koretsky AP, Dunbar CE (2003) Highly efficient endosomal labeling of progenitor and stem cells with large magnetic particles allows magnetic resonance imaging of single cells. Blood 102:867-872.

Ho C, Hitchens TK (2004) A non-invasive approach to detecting organ rejection by MRI: monitoring the accumulation of immune cells at the transplanted organ. Current pharmaceutical biotechnology 5:551-566.

Hoehn M, Kustermann E, Blunk J, Wiedermann D, Trapp T, Wecker S, Focking M, Arnold H, Hescheler J, Fleischmann BK, Schwindt W, Buhrle C (2002) Monitoring of implanted stem cell migration in vivo: a highly resolved in vivo magnetic resonance imaging investigation of experimental stroke in rat. Proc Natl Acad Sci U S A 99:16267-16272.

Janowski M, Walczak P, Kropiwnicki T, Jurkiewicz E, Domanska-Janik K, Bulte JW, Lukomska B, Roszkowski M (2014) Long-term MRI cell tracking after intraventricular delivery in a patient with global cerebral ischemia and prospects for magnetic navigation of stem cells within the CSF. PLoS One 9:e97631.

Jensen JH, Chandra R (2000) MR imaging of microvasculature. Magn Reson Med 44:224-230.

Jespersen SN, Bjarkam CR, Nyengaard JR, Chakravarty MM, Hansen B, Vosegaard T, Ostergaard L, Yablonskiy D, Nielsen NC, Vestergaard-Poulsen P (2010) Neurite density from magnetic resonance diffusion measurements at ultrahigh field: comparison with light microscopy and electron microscopy. Neuroimage 49:205-216.

Jiang Q, Zhang ZG, Chopp M (2010a) MRI of stroke recovery. Stroke 41:410-414.

Jiang Q, Zhang ZG, Chopp M (2010b) MRI evaluation of white matter recovery after brain injury. Stroke 41:S112-113.

Jiang Q, Gollapalli L, Haacke EM, Ding GL, Zhang ZG, Zhang L, Li L, Wang Y, Ewing JR, Hu J, Bagherebadian H, Chopp M (2008) Susceptibility Weighted MRI for Detection and Staging of Angiogenesis After Stroke in Rats. In: Proceedings of the Sixteenth Annual Meeting of the International Society for Magnetic Resonance in Medicine, pp 304. Toronto, Canada.

Jiang Q, Zhang ZG, Ding GL, Zhang L, Ewing JR, Wang L, Zhang R, Li L, Lu M, Meng H, Arbab AS, Hu J, Li QJ, Pourabdollah Nejad DS, Athiraman H, Chopp M (2005) Investigation of neural progenitor cell induced angiogenesis after embolic stroke in rat using MRI. Neuroimage 28:698-697-697.

Jiang Q, Qu C, Chopp M, Ding GL, Davarani SP, Helpern JA, Jensen JH, Zhang ZG, Li L, Lu M, Kaplan D, Hu J, Shen Y, Kou Z, Li Q, Wang S, Mahmood A (2011) MRI evaluation of axonal reorganization after bone marrow stromal cell treatment of traumatic brain injury. NMR Biomed 24:1119-1128.

Jiang Q, Zhang ZG, Ding GL, Silver B, Zhang L, Meng H, Lu M, Pourabdollah Nejad DS, Wang L, Savant-Bhonsale S, Li L, Bagher-Ebadian H, Hu J, Arbab AS, Vanguri P, Ewing JR, Ledbetter K, Chopp M (2006) MRI detects white matter reorganization after neural progenitor cell treatment of stroke. Neuroimage 32:1080-1089.

Kressler B, de Rochefort L, Liu T, Spincemaille P, Jiang Q, Wang Y (2010) Nonlinear regularization for per voxel estimation of magnetic susceptibility distributions from MRI field maps. IEEE Trans Med Imaging 29:273-281.

Krupinski J, Kaluza J, Kumar P, Kumar S, Wang JM (1994) Role of angiogenesis in patients with cerebral ischemic stroke. Stroke 25:1794-1798.

Li L, Jiang Q, Ding G, Zhang L, Zhang ZG, Li Q, Panda S, Lu M, Ewing JR, Chopp M (2010) Effects of administration route on migration and distribution of neural progenitor cells transplanted into rats with focal cerebral ischemia, an MRI study. J Cereb Blood Flow Metab 30:653-662.

Li Y, Liu Z, Xin H, Chopp M (2014) The role of astrocytes in mediating exogenous cell-based restorative therapy for stroke. Glia 62:1-16.

Li Y, Chen J, Wang L, Lu M, Chopp M (2001) Treatment of stroke in rat with intracarotid administration of marrow stromal cells. Neurology 56:1666-1672.

Li Y, Chopp M, Chen J, Wang L, Gautam SC, Xu YX, Zhang Z (2000) Intrastriatal transplantation of bone marrow nonhematopoietic cells improves functional recovery after stroke in adult mice. J Cereb Blood Flow Metab 20:1311-1319.

Li Y, Chen J, Zhang CL, Wang L, Lu D, Katakowski M, Gao Q, Shen LH, Zhang J, Lu M, Chopp M (2005) Gliosis and brain remodeling after treatment of stroke in rats with marrow stromal cells. Glia 49:407-417.

Lindvall O, Kokaia Z, Martinez-Serrano A (2004) Stem cell therapy for human neurodegenerative disorders-how to make it work. Nat Med 10 Suppl:S42-50.

Liu Z, Li Y, Qu R, Shen L, Gao Q, Zhang X, Lu M, Savant-Bhonsale S, Borneman J, Chopp M (2007) Axonal sprouting into the denervated spinal cord and synaptic and postsynaptic protein expression in the spinal cord after transplantation of bone marrow stromal cell in stroke rats. Brain Res 1149:172-180.

Lu D, Li Y, Wang L, Chen J, Mahmood A, Chopp M (2001) Intraarterial administration of marrow stromal cells in a rat model of traumatic brain injury. J Neurotrauma 18:813-819.

Medina-Kauwe LK, Xie J, Hamm-Alvarez S (2005) Intracellular trafficking of nonviral vectors. Gene Ther 12:1734-1751.

Melbourne A, Eaton-Rosen Z, Bainbridge A, Kendall GS, Cardoso MJ, Robertson NJ, Marlow N, Ourselin S (2013) Measurement of myelin in the preterm brain: multi-compartment diffusion imaging and multi-component T2 relaxometry. Med Image Comput Comput Assist Interv 16:336-344.

Mori S, van Zijl PC (2002) Fiber tracking: principles and strategies - a technical review. NMR Biomed 15:468-480.
Mouhieddine TH, Kobeissy FH, Itani M, Nokkari A, Wang KK (2014) Stem cells in neuroinjury and neurodegenerative disorders: challenges and future neurotherapeutic prospects. Neural Regen Res 9:901-906.
Mukherjee S, Ghosh RN, Maxfield FR (1997) Endocytosis. Physiol Rev 77:759-803.
Narayan RK, Michel ME, Ansell B, Baethmann A, Biegon A, Bracken MB, Bullock MR, Choi SC, Clifton GL, Contant CF, Coplin WM, Dietrich WD, Ghajar J, Grady SM, Grossman RG, Hall ED, Heetderks W, Hovda DA, Jallo J, Katz RL, et al. (2002) Clinical trials in head injury. J Neurotrauma 19:503-557.
NINDS (1995) The National Institute of Neurological Disorders and Stroke rt-PA Stroke Study Group: Tissue plasminogen activator for acute ischemic stroke. N Engl J Med 333:1581-1587.
O'Leary MT, Blakemore WF (1997) Oligodendrocyte precursors survive poorly and do not migrate following transplantation into the normal adult central nervous system. J Neurosci Res 48:159-167.
Ordidge RJ, Gorell JM, Deniau JC, Knight RA, Helpern JA (1994) Assessment of relative brain iron concentrations using T2-weighted and T2*-weighted MRI at 3 Tesla. Magn Reson Med 32:335-341.
Pathak AP, Schmainda KM, Ward BD, Linderman JR, Rebro KJ, Greene AS (2001) MR-derived cerebral blood volume maps: issues regarding histological validation and assessment of tumor angiogenesis. Magn Reson Med 46:735-747.
Risau W (1994) Molecular biology of blood-brain barrier ontogenesis and function. Acta Neurochir Suppl 60:109-112.
Risau W (1998) Development and differentiation of endothelium. Kidney Int Suppl 67:S3-6.
Schenker C, Meier D, Wichmann W, Boesiger P, Valavanis A (1993) Age distribution and iron dependency of the T2 relaxation time in the globus pallidus and putamen. Neuroradiology 35:119-124.
Shapiro EM, Skrtic S, Koretsky AP (2005) Sizing it up: cellular MRI using micron-sized iron oxide particles. Magn Reson Med 53:329-338.
Shen LH, Li Y, Chen J, Zhang J, Vanguri P, Borneman J, Chopp M (2006) Intracarotid transplantation of bone marrow stromal cells increases axon – myelin remodeling after stroke. Neuroscience 137:393-399.
Shimony JS, McKinstry RC, Akbudak E, Aronovitz JA, Snyder AZ, Lori NF, Cull TS, Conturo TE (1999) Quantitative diffusion-tensor anisotropy brain MR imaging: normative human data and anatomic analysis. Radiology 212:770-784.
Slevin M, Krupinski J, Slowik A, Kumar P, Szczudlik A, Gaffney J (2000) Serial measurement of vascular endothelial growth factor and transforming growth factor-beta1 in serum of patients with acute ischemic stroke. Stroke 31:1863-1870.
Song SK, Sun SW, Ramsbottom MJ, Chang C, Russell J, Cross AH (2002) Dysmyelination revealed through MRI as increased radial (but unchanged axial) diffusion of water. Neuroimage 17:1429-1436.
Sotak CH (2002) The role of diffusion tensor imaging in the evaluation of ischemic brain injury - a review. NMR Biomed 15:561-569.
Sun SW, Liang HF, Trinkaus K, Cross AH, Armstrong RC, Song SK (2006) Noninvasive detection of cuprizone induced axonal damage and demyelination in the mouse corpus callosum. Magn Reson Med 55:302-308.
Tuch DS, Reese TG, Wiegell MR, Wedeen VJ (2003) Diffusion MRI of complex neural architecture. Neuron 40:885-895.
Tuch DS, Reese TG, Wiegell MR, Makris N, Belliveau JW, Wedeen VJ (2002) High angular resolution diffusion imaging reveals intravoxel white matter fiber heterogeneity. Magn Reson Med 48:577-582.
Vymazal J, Brooks RA, Patronas N, Hajek M, Bulte JW, Di Chiro G (1995a) Magnetic resonance imaging of brain iron in health and disease. J Neurol Sci 134 Suppl:19-26.
Vymazal J, Hajek M, Patronas N, Giedd JN, Bulte JW, Baumgarner C, Tran V, Brooks RA (1995b) The quantitative relation between T1-weighted and T2-weighted MRI of normal gray matter and iron concentration. J Magn Reson Imaging 5:554-560.
Vymazal J, Brooks RA, Baumgarner C, Tran V, Katz D, Bulte JW, Bauminger R, Di Chiro G (1996) The relation between brain iron and NMR relaxation times: an in vitro study. Magn Reson Med 35:56-61.
Walczak P, Zhang J, Gilad AA, Kedziorek DA, Ruiz-Cabello J, Young RG, Pittenger MF, van Zijl PC, Huang J, Bulte JW (2008) Dual-modality monitoring of targeted intraarterial delivery of mesenchymal stem cells after transient ischemia. Stroke 39:1569-1574.
Wang S, Chopp M, Nazem-Zadeh MR, Ding G, Nejad-Davarani SP, Qu C, Lu M, Li L, Davoodi-Bojd E, Hu J, Li Q, Mahmood A, Jiang Q (2013) Comparison of neurite density measured by MRI and histology after TBI. PLoS One 8:e63511.
Watanabe T, Honda Y, Fujii Y, Koyama M, Matsuzawa H, Tanaka R (2001) Three-dimensional anisotropy contrast magnetic resonance axonography to predict the prognosis for motor function in patients suffering from stroke. J Neurosurg 94:955-960.
Wedeen VJ, Hagmann P, Tseng WY, Reese TG, Weisskoff RM (2005) Mapping complex tissue architecture with diffusion spectrum magnetic resonance imaging. Magn Reson Med 54:1377-1386.
Weiller C, Ramsay SC, Wise RJ, Friston KJ, Frackowiak RS (1993) Individual patterns of functional reorganization in the human cerebral cortex after capsular infarction. Ann Neurol 33:181-189.
Wu EX, Tang H, Jensen JH (2004) High-resolution MR imaging of mouse brain microvasculature using the relaxation rate shift index Q. NMR Biomed 17:507-512.
Xiong Y, Mahmood A, Chopp M (2010a) Angiogenesis, neurogenesis and brain recovery of function following injury. Curr Opin Investig Drugs 11:298-308.
Xiong Y, Mahmood A, Chopp M (2010b) Neurorestorative treatments for traumatic brain injury. Discov Med 10:434-442.
Xu XL, Yi F, Pan HZ, Duan SL, Ding ZC, Yuan GH, Qu J, Zhang HC, Liu GH (2013) Progress and prospects in stem cell therapy. Acta Pharmacol Sin 34:741-746.
Zelivyanskaya ML, Nelson JA, Poluektova L, Uberti M, Mellon M, Gendelman HE, Boska MD (2003) Tracking superparamagnetic iron oxide labeled monocytes in brain by high-field magnetic resonance imaging. J Neurosci Res 73:284-295.
Zhang L, Zhang RL, Wang Y, Zhang C, Zhang ZG, Meng H, Chopp M (2005) Functional recovery in aged and young rats after embolic stroke: treatment with a phosphodiesterase type 5 inhibitor. Stroke 36:847-852.
Zhang R, Chopp M, Zhang ZG (2013) Oligodendrogenesis after cerebral ischemia. Front Cell Neurosci 7:201.
Zhang R, Wang Y, Zhang L, Zhang Z, Tsang W, Lu M, Chopp M (2002a) Sildenafil (Viagra) induces neurogenesis and promotes functional recovery after stroke in rats. Stroke 33:2675-2680.
Zhang R, Wang L, Zhang L, Chen J, Zhu Z, Zhang Z, Chopp M (2003a) Nitric oxide enhances angiogenesis via the synthesis of vascular endothelial growth factor and cGMP after stroke in the rat. Circ Res 92:308-313.
Zhang RL, Zhang L, Zhang ZG, Morris D, Jiang Q, Wang L, Zhang LJ, Chopp M (2003b) Migration and differentiation of adult rat subventricular zone progenitor cells transplanted into the adult rat striatum. Neuroscience 116:373-382.
Zhang ZG, Chopp M (2009) Neurorestorative therapies for stroke: underlying mechanisms and translation to the clinic. Lancet Neurol 8:491-500.
Zhang ZG, Zhang L, Jiang Q, Chopp M (2002b) Bone marrow-derived endothelial progenitor cells participate in cerebral neovascularization after focal cerebral ischemia in the adult mouse. Circ Res 90:284-288.
Zhang ZG, Jiang Q, Zhang R, Zhang L, Wang L, Arniego P, Ho KL, Chopp M (2003c) Magnetic resonance imaging and neurosphere therapy of stroke in rat. Ann Neurol 53:259-263.
Zhang ZG, Zhang L, Tsang W, Soltanian-Zadeh H, Morris D, Zhang R, Goussev A, Powers C, Yeich T, Chopp M (2002c) Correlation of VEGF and angiopoietin expression with disruption of blood-brain barrier and angiogenesis after focal cerebral ischemia. J Cereb Blood Flow Metab 22:379-392.